Geophysical Journal International

Geophys. J. Int. (2010) **180,** 703–714 doi: 10.1111/j.1365-246X.2009.04458.x

FAST TRACK PAPER

Evidence of active backthrusting at the NE Margin of Mentawai Islands, SW Sumatra

Satish C. Singh,[1] Nugroho D. Hananto,[1] Ajay P. S. Chauhan,[1] H. Permana,[2] Marine Denolle,[1] Andri Hendriyana[1] and Danny Natawidjaja[2]

[1] *Laboratoire de Géosciences Marines, Institut de Physique du Globe de Paris,* 4 *place Jussieu,* 75252 *Paris Cedex* 05, *France. E-mail: singh@ipgp.fr*
[2] *LIPI, Jl. Sangkuriang, Bandung* 40132, *Indonesia*

Accepted 2009 November 17. Received 2009 November 4; in original form 2009 April 23

SUMMARY

The Indo-Australian plate subducts obliquely beneath the Sunda plate leading to a slip partitioning into pure thrust and strike-slip motion. Just in the last 5 yr, three pure thrust earthquakes of $M_w > 8.4$ have occurred along this subduction interface. The Great Sumatra Fault, traversing the Sumatra continental block, takes up a significant part of the strike-slip motion, but the Mentawai Fault bounding the NE margin of Mentawai Islands has been suggested to accommodate a part of the strike-slip motion. Although the great Sumatra Fault is active, no seismicity has been observed along the Mentawai fault. Using a combination of high-resolution seismic reflection and bathymetry data, here we show that the Mentawai Fault seems to be characterized by active SW dipping backthrusts. The presence of recent steeply dipping thrust earthquakes suggests that these faults should be active. Combined with results from north in 2004 earthquake region and south of this study area, our results suggest that backthrusting should play an important role in forearc evolution SW of Sumatra. We also observed several mass wasting sites at NE margin of the Mentawai Islands, which could be erosional features or landslides triggered by earthquake activities. Localized uplift along the steeply dipping backthrusts at the NE margin of Mentawai Islands in the fully locked region could pose serious seismic and tsunami risks to the SW coast of Sumatra in the future.

Key words: Tsunamis; Seismicity and tectonics; Subduction zone processes; Continental margins: convergent; Submarine landslides.

1 INTRODUCTION

The Sumatra subduction system is a classic example of oblique convergence and slip partitioning as the Indo-Australian plate subducts beneath the Burmese plate. The plate convergence rate is ∼60 mm yr^{-1} and orthogonal to the subduction front near Java, which reduces to 52 mm yr^{-1} in the Northern Sumatra with an obliquity of about 40° and becomes dominantly trans-current north of Nicobar Island (Prawirodirdjo 2000; Prawirodirdjo *et al.* 2000) with some convergence. Fitch (1972) suggested that the dextral component of the relative motion between the two plates is accommodated by a trench-parallel strike-slip fault system. The seismic activity and the linear shape of the Great Sumatra Fault (GSF) seem to accommodate a significant part of the dextral motion (McCaffrey *et al.* 2000). The 1900-km-long GSF traverses the continental block, roughly following the active Sumatran volcanic arc. Recent GPS studies show a slip rate of ∼10 mm yr^{-1} south of the equator that increases rapidly to 27 mm yr^{-1} along the northern part of the GSF (Bellier *et al.* 1999; Sieh & Natawidjaja 2000). The subduction front and the GSF are separated by a 300-km-wide forearc deformation zone that includes about 60-km-wide active accretionary prism, Mentawai Islands (or forearc ridges) and 150-km-wide Mentawai forearc basin.

Based on a single channel seismic reflection study, Diament *et al.* (1992) suggested that the northeastern margin of the Mentawai Islands might be a site for a secondary strike-slip fault, the Mentawai Fault. Their interpretation was based on unmigrated seismic data that indicated flower-like structures, which are generally attributed to be due to strike-slip faults. Schluter *et al.* (2002) and Kopp *et al.* (2001) have also imaged push-up ridges within the Mentawai forearc basin, having flower structures indicating the presence of a strike-slip fault. The presence of a secondary strike-slip fault bounding the forearc basin also explained the difference in slip rates between the northern and southern parts of the GSF. The linearity of the NE border of the Mentawai Islands further supported the possibility of a strike-slip fault along the margin, and hence it has become accepted paradigm that the Mentawai Fault is of a strike slip nature. However, there has been no strike-slip earthquake along the

Mentawai Fault in the last 30 yr. Furthermore, recent GPS data do not show any lateral motion between the Mentawai Islands and mainland Sumatra, which along with the lack of strike-slip earthquakes in the region led Natawidjaja *et al.* (2006) to suggest that the Mentawai strike-slip fault has not been active for the last several thousand years. To study the role the Mentawai Fault might play in seismic and tsunami risk assessment, the Pre-Tsunami Investigation of Seismic Gap (Pre-TIGap) survey was carried out as a part of the French-Indonesian cooperation involving Institut de Physique du Globe de Paris and the Indonesian research agencies (LIPI, BPPT and MGI). In this paper, we present seismic reflection and bathymetric images and interpret them along with other geological and geophysical results.

2 Pre-TIGap 2008 EXPERIMENT

High-resolution bathymetry and multichannel seismic data were acquired on board the LIPI research vessel Baruna Jaya VIII from 2008 February 15 to March 6. Seismic reflection data was acquired using a 28-channel 750-m-long streamer at a group interval of 25 m. Source consisted of four sleeve guns providing a total volume of 530 cubic inches at 1600 psi pressure and was fired every 25 m, leading to a CDP bin spacing of 12.5 m. A total of 14 dip lines were shot at 10–20 km intervals along the 350 km long northeastern margin of Siberut-Sipora-Pagai Islands (Fig. 1). The length of the lines varied from 20 to 40 km in water depth up to 1700 m. The data were processed using standard processing sequence, for example, noise removal, common mid point (CMP) binning, velocity analysis and stacking. Since we had a short offset streamer, the velocity was poorly estimated, and therefore we performed a constant velocity (1500 m s^{-1}) post-stack frequency wave number migration to remove the diffraction effects.

The bathymetric data was acquired using EM1002, providing horizontal and vertical resolutions of 3–5 and 1 m, respectively, in water depths range from 50 to 1100 m. Single beam data allowed us to extend the bathymetric data to deeper waters. Over 900 km^2 of bathymetric data were acquired in five boxes, covering areas around the seismic profiles in order to link surface morphological features with structures at depth (Fig. 1).

3 BACKTHRUSTS

Four uninterpreted and interpreted seismic profiles from NW to SE are shown in Figs 2 and 3, respectively, along with 2-km-wide strips of bathymetry. The northernmost profile 13 is at the northeastern margin of the Siberut Island (Figs 2a and 3a). Near the coast, towards SW end of the profile, between CMP 150 and 600, a thick (up to 1750 ms) synclinal piggyback basin is imaged, which is bounded by an asymmetric anticline (push-up ridge) in the NE. A backthrust is imaged that seems to control the uplift of the push-up ridge and dams the piggyback basin, which is clearly visible on the bathymetric strip. Further northeastwards, the basin shows a general evolution of a subsiding forearc basin, that is, thickening of sediments towards NE without any near surface extensional

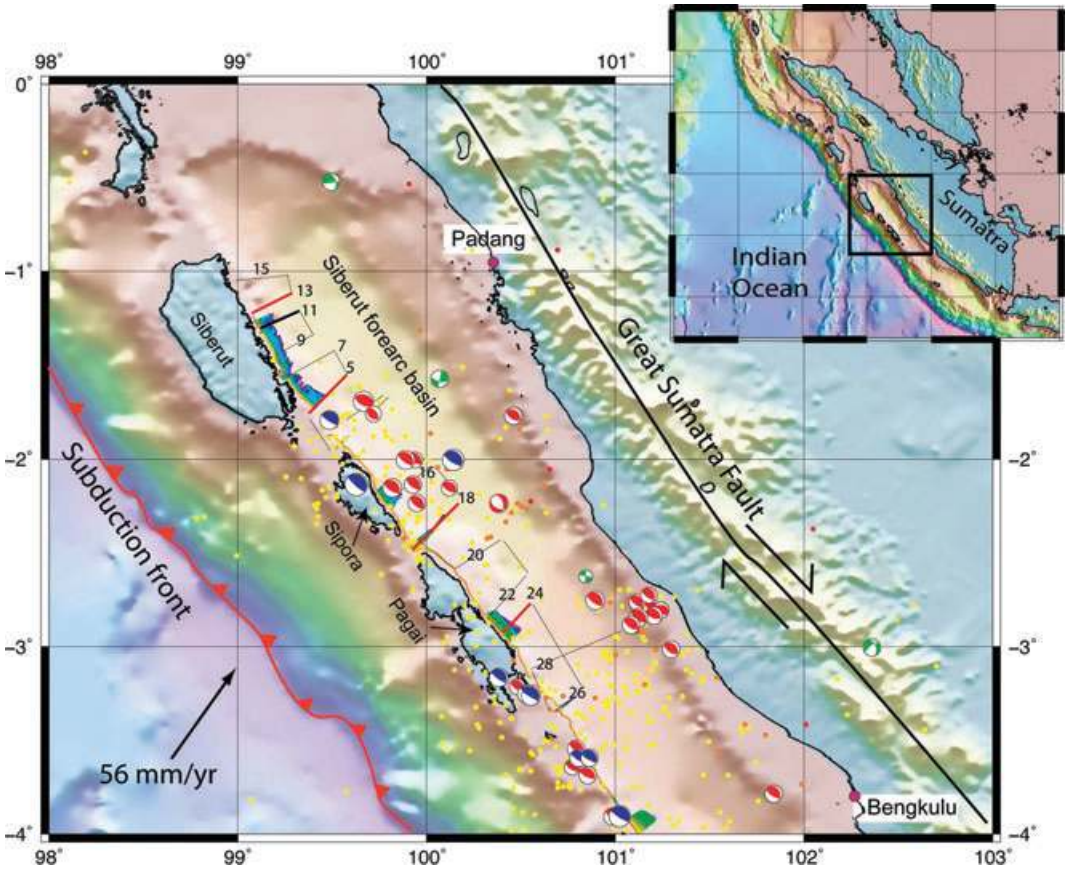

Figure 1. Pre-TIGap study area. Seismic reflection profiles are shown in light grey lines, those shown in Fig. 2 in red and that in Fig. 3 in black. New high-resolution bathymetry at NE margin of Mentawai Islands is in dark colours. The shallow dipping earthquakes with $M_w > 5$ are shown by blue beach balls and steeply dipping events by red beach balls. The locations are from Engdahl *et al.* (2007) and the focal mechanism from Harvard CMT solution. Coloured circles are the aftershocks of 2007 earthquake. The Inset shows the location of study area.

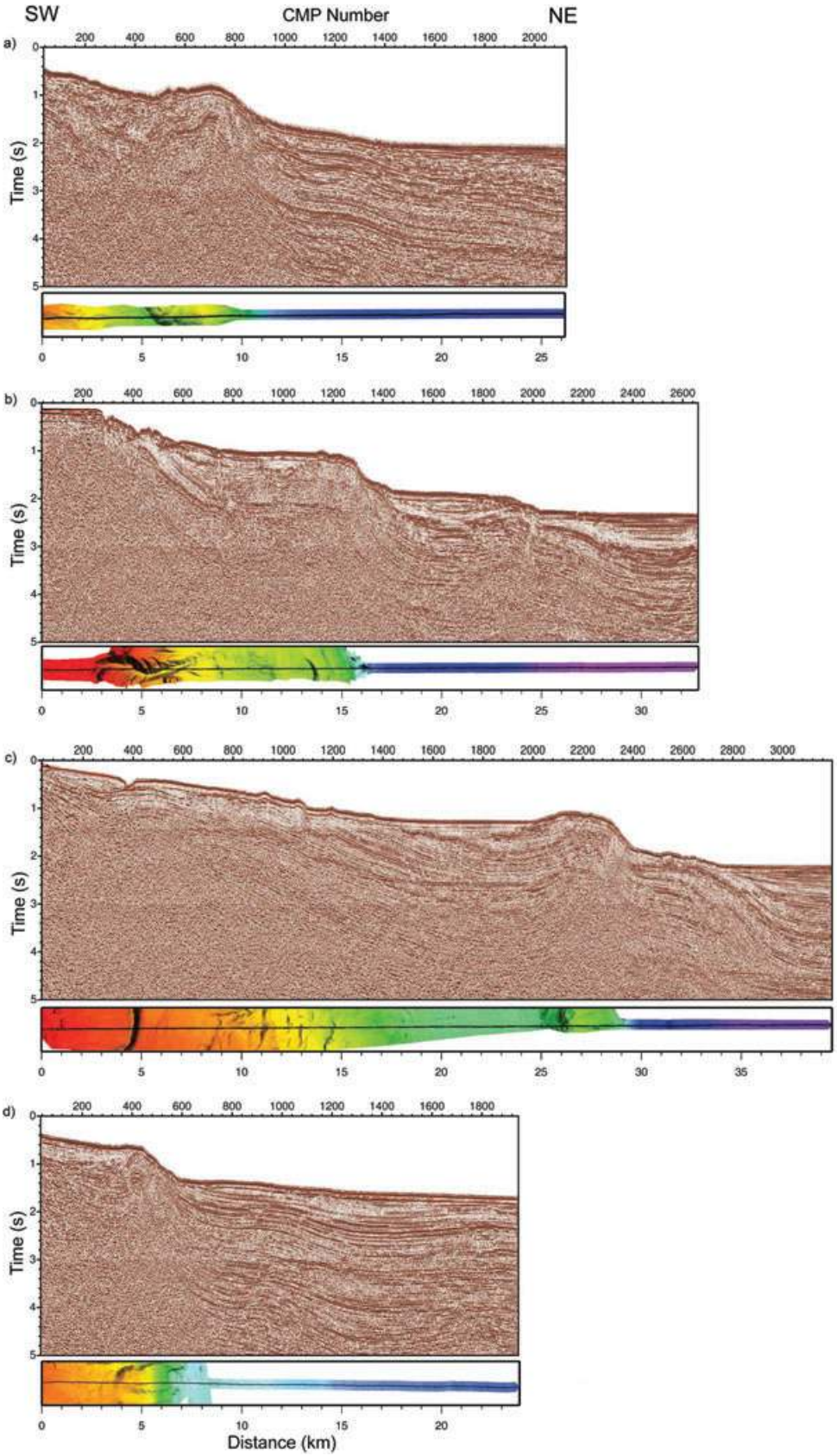

Figure 2. Seismic images: Uninterpreted seismic reflection profiles from north to south: (a) 13, (b) 5, (c) 18 and (d) 24 along with 2.0 km bathymetry strips along these profiles. Vertical to horizontal scale is 1:4. See Fig. 1 for location of profiles.

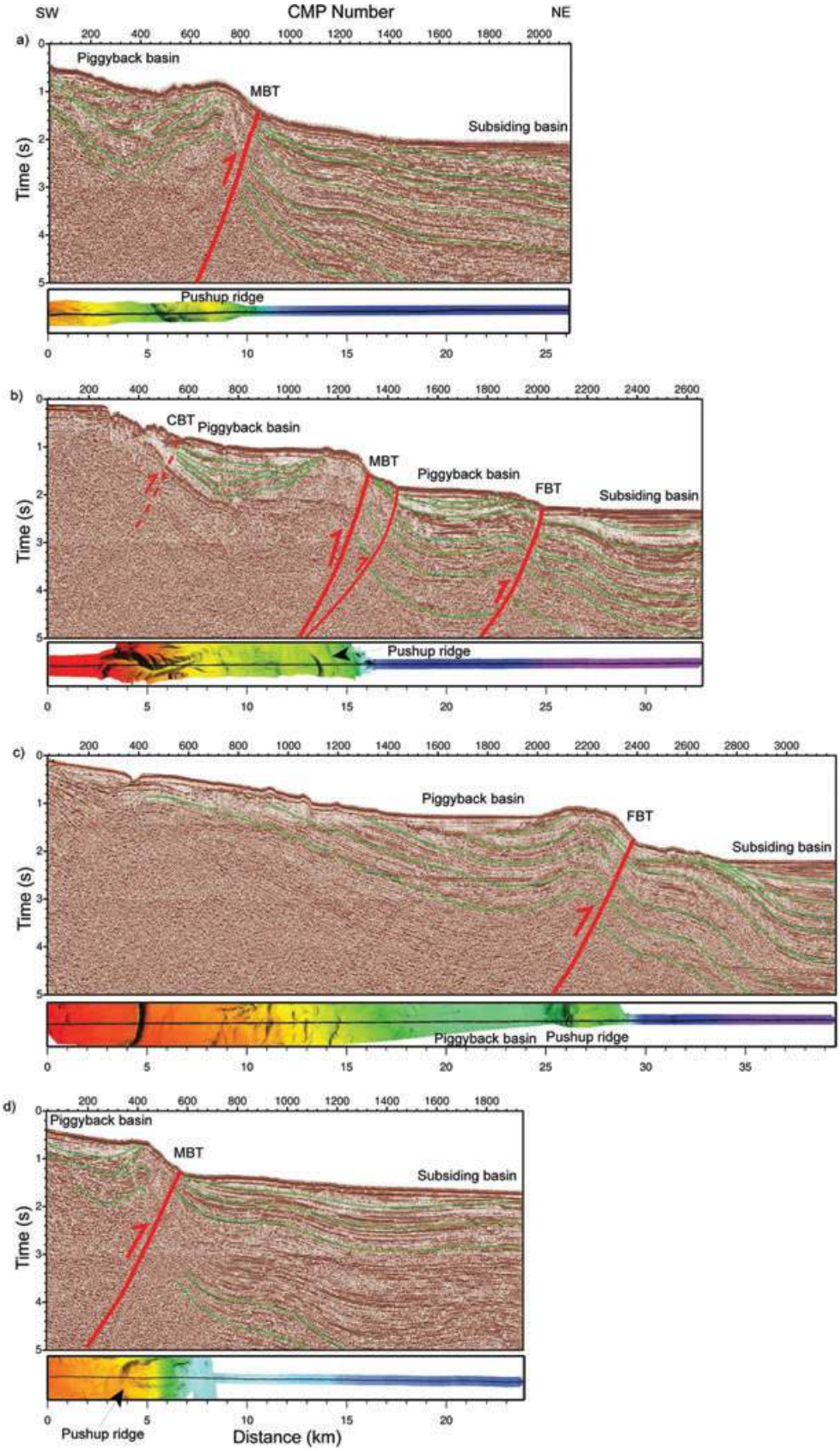

Figure 3. Seismic images: Interpreted seismic reflection profiles from north to south: (a) 13, (b) 5, (c) 18 and (d) 24 along with 2.0 km bathymetry strips along these profiles. Backthrusts are marked in red. MBT: main backthrust, FBT: frontal backthrust. FBT is imaged along profiles 1, 3, 5, 11, 16 and 18. Vertical to horizontal scale is 1:4. See Fig. 1 for location of profiles.

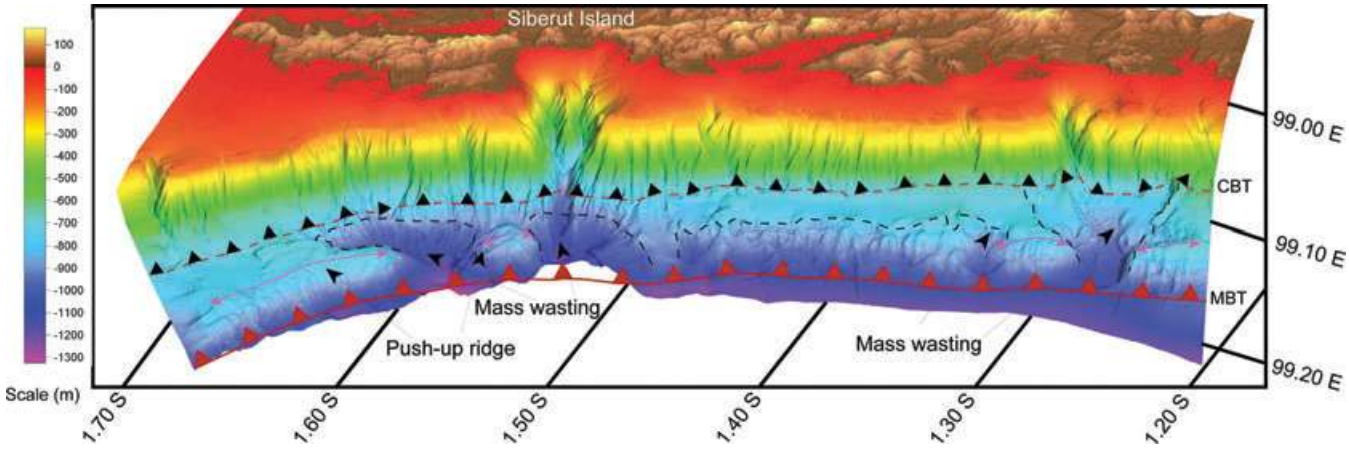

Figure 4. Bathymetry: 3-D view of bathymetry NE of Siberut Island. MBT: main backthrust (red), CBT: coastal backthrust (black). Push-up ridges are marked by purple arrows and dashed black line bounds mass wasting.

faulting. Two types of deformation are observed in this region: gentle folding and northeastward tilting of deeper sediments, suggesting a large-scale (basin-scale) deformation, and nearly flat upper 300 ms sediments reflecting recent subsidence. Profile 15 (Fig. 1), which is 18 km further northwest, shows similar features.

Profile 5 (Figs 2b and 3b) is at the southern end of the Siberut Island at 65 km SE of profile 13 and shows two terraces of synclinal piggyback basins, bounded by asymmetric anticlinal push-up ridges. The coastal piggyback basin is similar to that imaged on profile 13, but has thicker recent sediments. The synclinal nature of the folded sediments in these basins suggests that they are produced by back thrusting and folding, not by tilting of normal fault blocks. On the NW side, the piggyback basin is bounded by a backthrust controlling the uplift of the island, which we call coastal back thrust (CBT). In NE, the piggyback basin and the associated anticlinal push-up ridge are uplifted by two backthrusts that arrive on the seafloor near the slope breaks. Further northeastwards, the second piggyback basin at a water depth of 1300 m is also 5.5 km wide (CDP 1440-1880), but consists of much thicker folded sediments, and is bounded by a SW dipping active thrust fault at its NE side. This thrust fault is localized and has been imaged around profiles 5 and 11, but is absent on profile 7, and could be considered as a frontal thrust/fold (FBT), similar to the frontal thrust observed near the subduction front (Singh *et al.* 2008). Therefore, we suggest that the thrust bounding the first piggyback basin with a high bathymetric relief (600 m) is the main backthrust (MBT).

Profile 18 (Figs 2c and 3c) was shot between Sipora and North Pagai Islands, at about 100 km SE of profile 5. An eroded piggyback basin above an unconformity is imaged (CMP 150-950). A well-developed piggyback basin and an asymmetric push-up ridge are present. The upper sediments in the piggyback basin are horizontal above thick folded and deformed sediments. The push-up ridge seems to consist of older and deformed sediments. A clear backthrust (FBT) is observed at the slope break NE of the push-up ridge. Just NE of the FBT, sediments show signs of folding, which could be due to a blind thrust at depth or rapid increase of subsidence northeastwards. The MBT is not well imaged along this profile. Profile 16, which is about 30 km NE, shows similar piggyback basin and FBT but also the MBT and the associated piggyback basin, suggesting that MBT should be present until profile 16.

Profile 24 (Figs 2d and 3d) is at the NE margin of South Pagai Island. It shows a piggyback basin, bounded by a push-up ridge and associated MBT. Profiles 20 and 22, respectively 20 and 35 km NW of profile 24, show similar features, suggesting that the deformation is mainly localized at MBT, which is imaged over a significant part (350 km) of the NE Mentawai Islands. The CBT might be present, but is poorly imaged.

Profile 26 is about 60 km SE of profile 24, south of the chain of Mentawai Islands. It shows a backthrust at the slope break at 700 m water depth and a 6-km-wide local basin, which might be the piggyback basin. Our profiles do not cross the whole forearc basin, and therefore, it is possible that there could be other structures further NE of our profiles that might accommodate strike-slip motion.

4 BATHYMETRIC IMAGE

The bathymetry data allow us to determine the lateral continuity of the features observed on the seismic profiles along the whole margin (Figs 4 and 5). The bathymetric data clearly show a carbonate platform at 60–100 m water depth, which might be the shoreline formed during the last glacial maximum. The water depth suddenly increases to 600 m with a steep slope (30°), which shows a strong erosional features and canyons. The CBT is clearly visible at the slope break around 650 m water depth. The 5–6 km wide nearly flat basin (piggyback) is observed all along the margin (Fig. 4), which is bounded by a push-up ridge and the associated MBT. The bathymetry near Sipora Island (Fig. 5a) also shows the carbonate platform at 60–100 m water depth and CBT at the slope break at 600 m water depth. The piggyback basin and push-up ridge could also be seen. The first slope break at the South Pagai Island (Fig. 5b) is at shallower water depth (400 m) but the piggyback basin and push-up ridge can be clearly identified. There is a second slope break at 1100 m water depth, which should corresponds to the MBT. The combined bathymetry and seismic reflection data suggest that there are three backthrusts along the NE margin of Mentawai Island. The amount of vertical displacement along these faults is variable along the margin.

5 MASS WASTING

The bathymetric data also show some mass wasted region at the NE margin of Siberut Island (Fig. 4). Two of them are associated with canyons, and others are not, and hence they could be produced either by a long-term erosional process or during mass wasting. The push-up ridge seems to have been chopped off by mass wasting between 1.30°S and 1.50°S tick marks. The sharpness of the walls in some of the mass wasted regions suggests that some material might

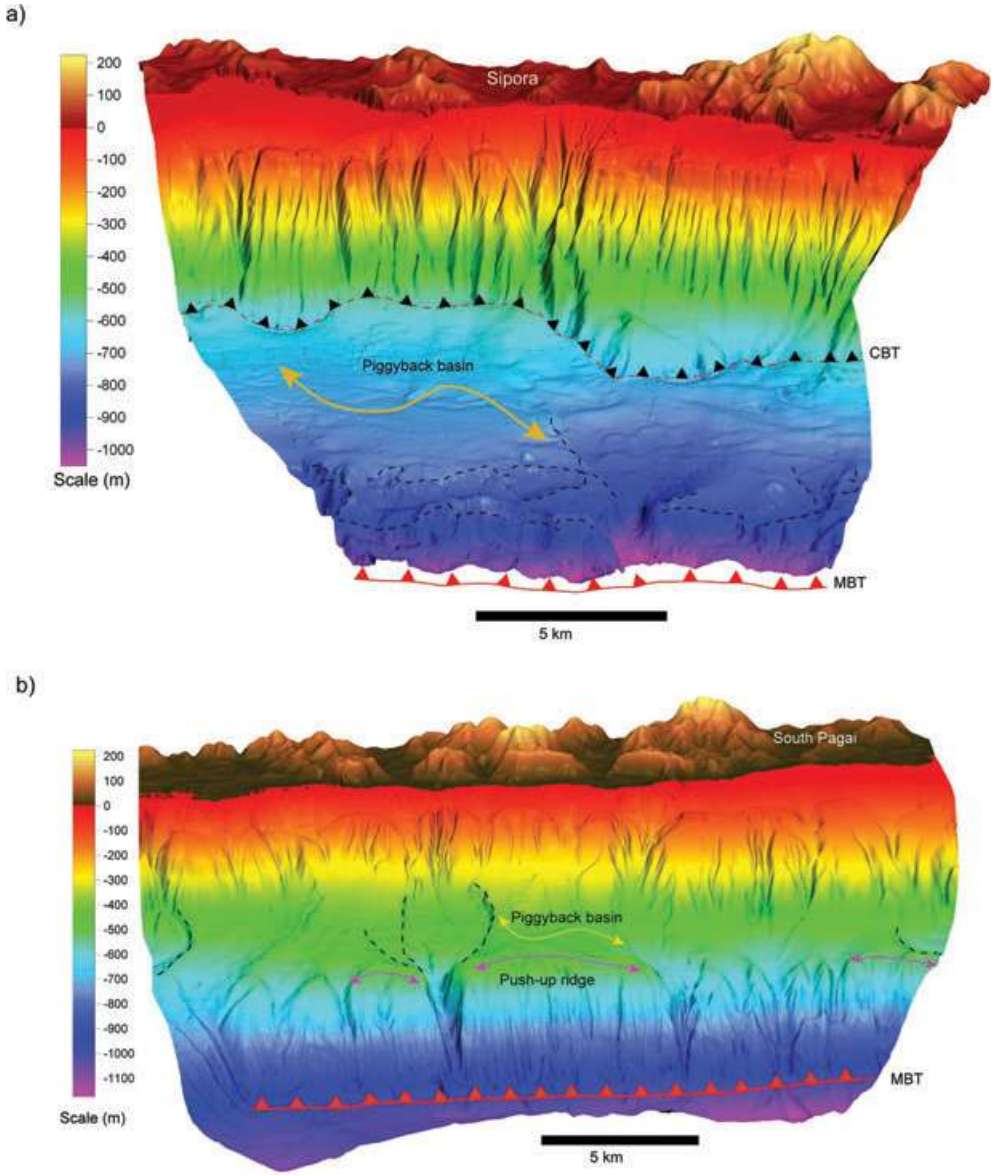

Figure 5. Sipora and South Pagai Islands bathymetry: Interpreted bathymetry at NE margin of Sipora (a) and South Pagai (b) Islands. See Fig. 1 for the location of survey area.

have been removed during landslides. The poor reflective layers between sedimented layers on seismic images (e.g. Figs 2b and 3b) suggest the existence of large mass wasted material that could only have been produced by turbiditic sequence and should be due to mass wasting. Layering in this poor reflective zone could have been produced by different episodes of mass wasting. A triangle-shaped (8–10 km) mass wasted region is observed at NW of the survey area around seismic profile 11 (1.35° S; Fig. 6). The seismic reflection profile going through the mass wasted region (Figs 6b and c) shows the absence of the main push-up ridge and the upper sediments of the piggyback basin, suggesting that significant part of the sediments have been removed. It also shows a thick layer of poor reflective sediments, which are likely to have been deposited during mass wasting, and therefore, we suggest that this mass wasted region is produced during mass wasting. The age of the mass wasting is difficult to determine from seismic and bathymetric data. The seismic image also shows the FBT and associated piggyback basin that contains about 500 ms thick layer of poor reflective sediments (orange colour), which could be debris flow (Fig. 6c). If we assume that the initial bathymetry was the same as that along profile 5, a 500 ms of sediments should have been removed in this area. If we assume a sediment velocity of 1.7 km s^{-1}, 6 (=0.42 × 15) km^3 of sediments would have been mobilized during the mass wasting. Our initial modelling results show that 50 cm high local waves could be generated during a sudden failure of this region. Seismic profile 7 traverses another mass wasted region at 1.50°S and shows similar features as profile 11. A 200–300 ms thick poor reflective sedimentary sequence is also imaged on profile 5 (Figs 2b and 3b) beneath 300–500 ms the seafloor, which could be due to previous mass wasting sequence. Small mass wasted regions are observed near profiles 16 and 24 (Fig. 5). Although the total amount of sediments observed in these mass wasted regions is small (∼30 km^3), these combined with back thrust could produce large localized tsunami if mobilized simultaneously. There are about 600 km^3 of unconsolidated sediments present in the piggyback basins bounded by the push-up ridges on the SW margin of the Siberut basin (Fig. 8a),

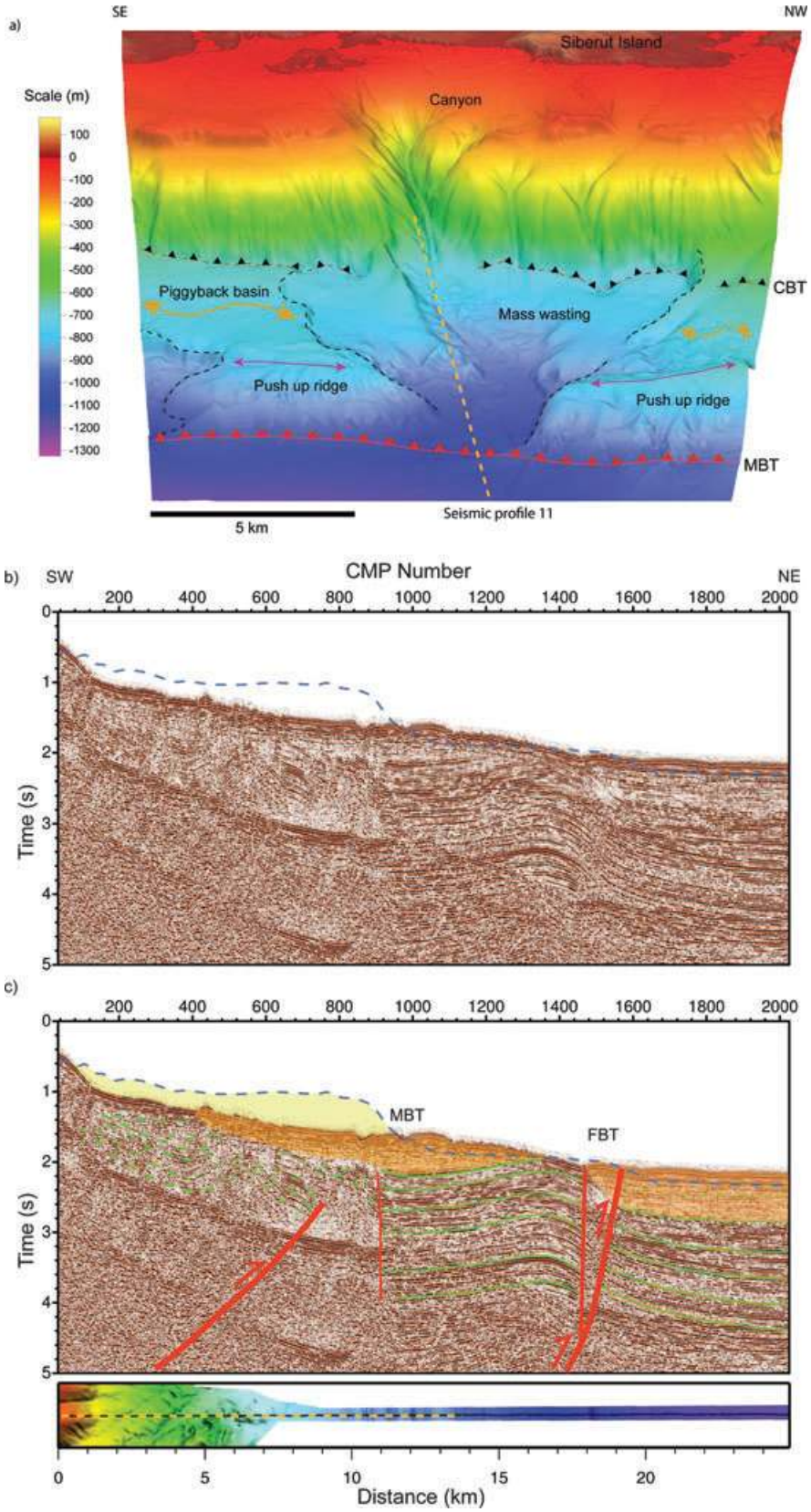

Figure 6. Mass wasting: (a) 3-D view of the mass wasting near 1.25°S on Fig. 4. Black dashed lines mark boundary of mass wasted regions, purple arrows push-up ridges, mustard colour arrows piggyback basins. Uninterpreted (b) and interpreted (c) seismic profile 11 traversing the mass wasted region. Blue dashed curve shows the seafloor on profile 5 (Fig. 3b), yellow area is the difference between seafloor on profiles 5 and 11, possibly mass wasted, and brown coloured zone shows low reflectivity sediments, possibly debris flow. The portion of profile 11 on two images is marked by mustard colour dashed line.

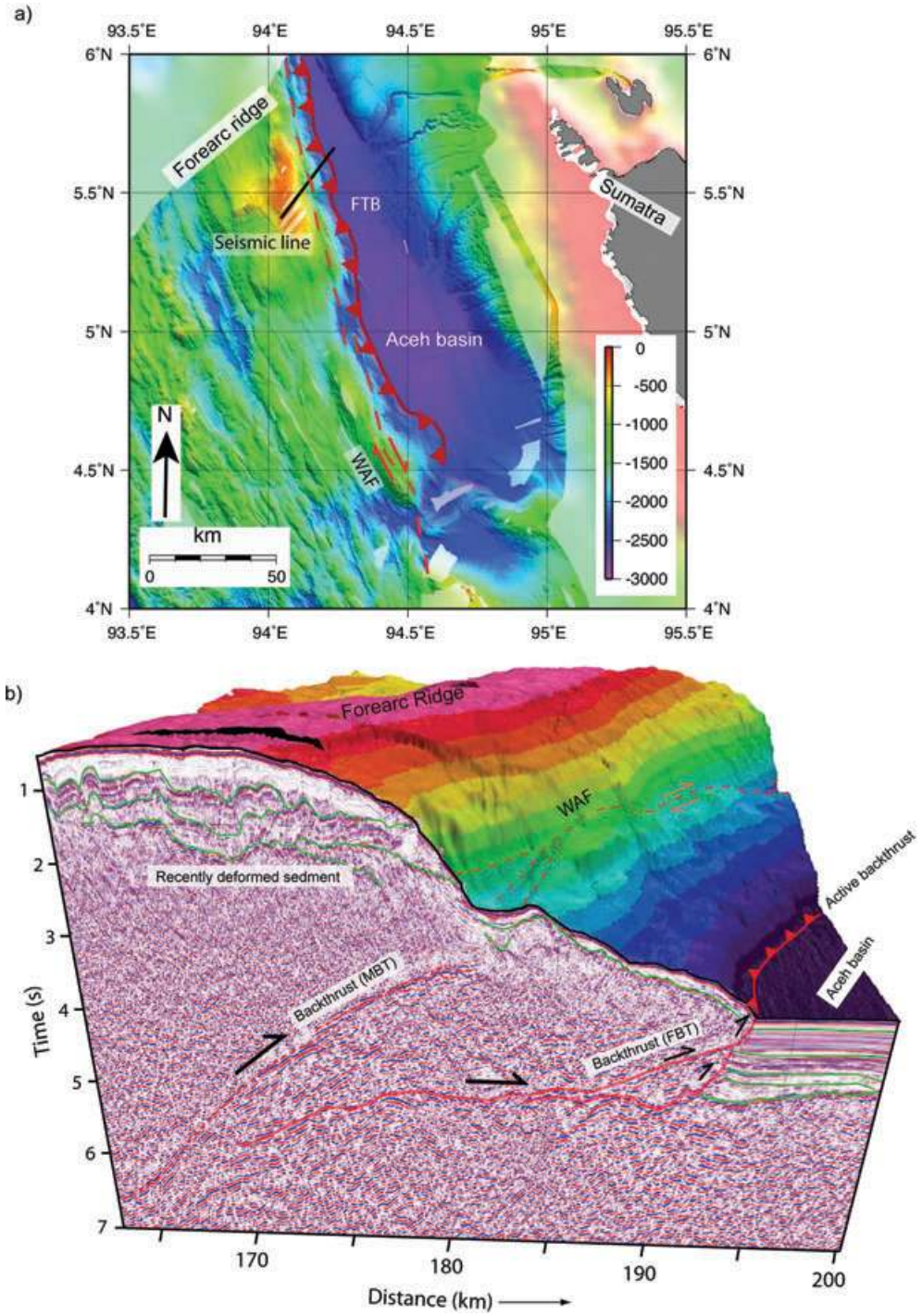

Figure 7. Deep seismic image: (a) seafloor bathymetry around Aceh forearc basin, forearc ridge and interpreted FBT. The red dashed curve indicates the position of strike-slip WAF identified by Singh *et al.* (2005). (b) 3-D block diagram showing deep seismic reflection image and bathymetry along black line shown in Fig. 7(a). FBT is frontal thrust fault and MBT is main backthrust. WAF seems to branch out into three branches forming a pull-apart basin above MBT.

which could generate a large tsunami, if mobilized instantaneously. Further modelling is required to quantify the size of tsunami that could be generated and is the subject of a future study.

6 DISCUSSION

Some normal faulting is observed along our profile (e.g. Fig. 6c) that might be associated with strike-slip motion, however, most of our profiles show the presence of an active back thrusting on the NE margin of Mentawai Islands. The shallow seismic reflection data permit the imaging of these faults down to a couple of kilometres below the seafloor; they should be connected at depth in a manner similar to the backthrusts imaged north of Simeulue Island (Singh *et al.* 2008; Chauhan *et al.* 2009). In the north near 5°35′N (Fig. 7), we have imaged the backthrust down to 7 s two-way traveltime (15 km). Folded and faulted sediments over highly compacted

sediments suggest that the forearc ridge has recently been uplifted (Fig. 7). This backthrust seems to have two branches, the lower one arriving at SW margin of the Aceh basin (FBT), and the upper one (MBT) terminating at depth where the West Andaman Fault (WAF) has been identified from bathymetry (Singh *et al.* 2005; Sibuet *et al.* 2007; Graindorge *et al.* 2008) and high-resolution shallow seismic (Seeber *et al.* 2007; Mosher *et al.* 2008) data. It is possible that the WAF, which is a right-lateral strike-slip fault, is a near surface manifestation of the upper backthrust, accommodating some transpressional motion (Chauhan *et al.* 2009). The presence of a small pull-apart basin above the MBT (Fig. 7b) suggests that this might be the case. In the same region but further south, Singh *et al.* (2008) have imaged a push-up ridge at about 55 km SW of a backthrust, which they associate with the WAF. South of our study area around 6°S, Schluter *et al.* (2002) have imaged a push-up ridge having a flower structure, suggestive of the presence of a strike-slip fault. However, they have also imaged a seaward dipping reflection just SW of the push-up ridge, which might be the manifestation of a backthrust at depth, and the push-up ridge might be the near surface expression of transpressional motion. In the same region, Kopp *et al.* (2001) have also imaged a similar push-up ridge. These results along with our results suggest that the seaward dipping backthrusting seems to be present along most of the NE margin of forearc ridges and Islands in SW Sumatra. However, there seems to be an intricate relationship between backthrusting and strike-slip faulting in the Sumatra forearc basin, and more deep seismic reflection data are required in this region to address this relationship.

It is difficult to date the activity along the backthrusts, but the presence of old deformed sediments on the main push-up ridges, recent sediments in the piggyback basins and the high bathymetric relief of the push-up ridges (up to 600 m) suggest that MBT has been active in the recent past. More than ten thrust earthquakes of $M_w >$ 5.0 with dip $>30°$ have occurred in the region since 2005, suggesting that the back thrust is indeed active (Fig. 1). The epicentres of these events mainly lie along the NE margin of Mentawai Islands, in 15–25 km depth range (Fig. 8). The recent GPS data from the

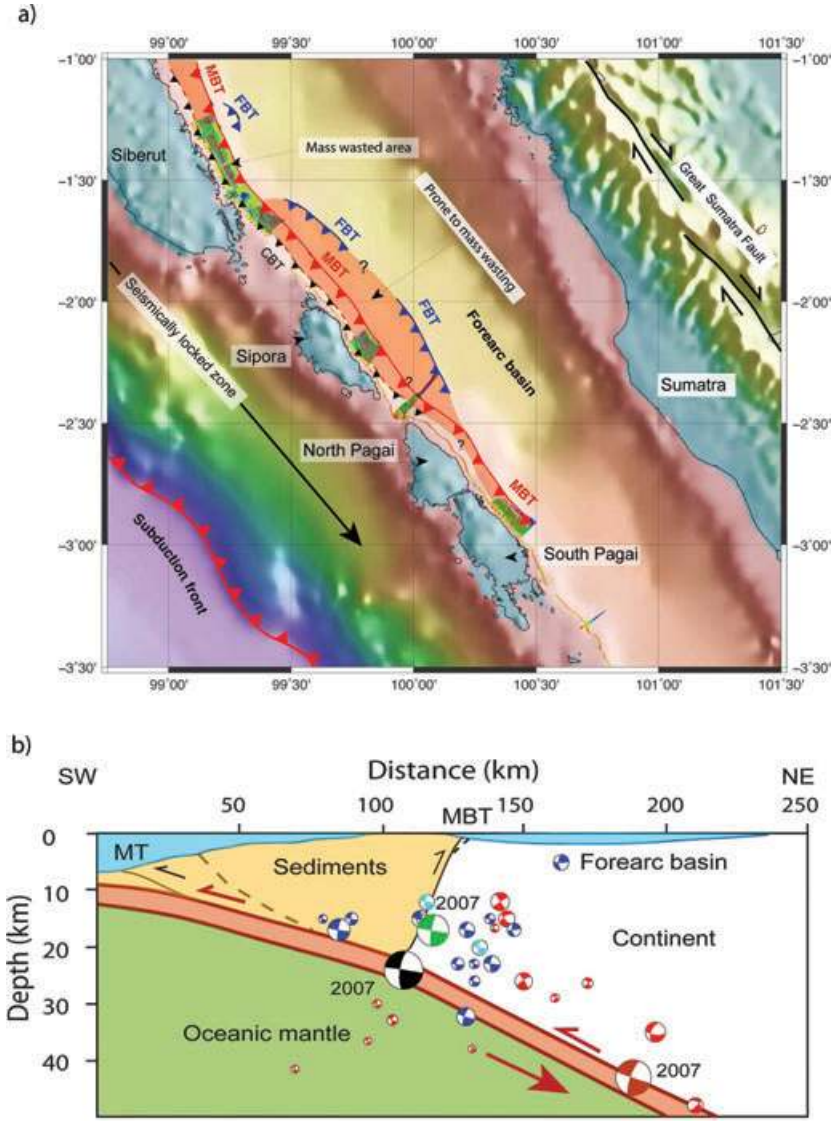

Figure 8. Backthrusts and mass wasted area: (a) map showing the location of backthrusts (red) and observed mass wasted region (green) in the study area. Light red colour is the area prone to future mass wasting (600 km^3). (b) Schematic cross-section showing downgoing oceanic crust (brown), megathrust (MT) and backthrust, based on Kopp *et al.* (2002) velocity model. Black (8.4), brown (7.9) and green (7.0) beach balls indicate the projection of the 2007 September megathrust sequence. Blue and red beach balls are shallow dipping and steeply dipping aftershocks, respectively. Light blue beach balls are projected hypocentres for 2008 earthquakes.

islands suggest that these islands move only normal to the subduction front and have no trench parallel motion (Chlieh *et al.* 2008). Furthermore, there have been no strike-slip earthquakes along the Mentawai fault zone in the last 30 yr (Natawidjaja *et al.* 2006). Our results combined with these observations suggest that the Mentawai fault zone should consist primarily of active backthrusts.

A shallow megathrust earthquake of $M_w = 8.4$ occurred on 2007 September 12 at the southern extremity of our study area (Fig. 8b). It was a shallow dipping event initiated beneath the forearc ridge, which seems to have broken the upper part of the locked zone (Lorito *et al.* 2008). Twelve hours later, a second event of $M_w = 7.9$ occurred at ∼43 km depth that seems to have broken the lower part of the locked zone; the boundary between the two rupture areas is at the NE margin of South Pagai Island (Konca *et al.* 2008). A third event of $M_w = 7.0$ occurred four hours later and seems to project along the interpreted backthrust (Fig. 8b). Recently, an earthquake of magnitude $M_w = 6.3$ occurred at 10 km depth on 2008 November 22, which also projects near the backthrust. Although the hypocenter of these earthquakes has a large uncertainty, the general trend of depth profile gives some idea about the possible activity on the backthrust.

The coral data have been used to estimate coseismic and interseismic uplift and subsidence for the past 750 yr in the Mentawai Island region (Natawidjaja *et al.* 2006, 2007; Sieh *et al.* 2008). The absence of any coral data on the SW margin of Siberut Island does not permit to say anything about the possible role of backthrust. However, coral data are available on both sides of Sipora and Pagai Islands. The overall uplifts were slightly higher towards SW than NE margins of these islands during the 1797 and 1833 earthquakes, suggesting the major uplift was due to megathrust, but that does not rule out the possibility of some uplift along the backthrust. The interseismic subsidence for the last 50 yr shows complex behaviour on Sipora Island (Natawidjaja *et al.* 2007), but slightly higher subsidence at SW margin of Pagai Islands. Therefore, the coral data do not provide any conclusive evidence for the presence of backthrust.

Chlieh *et al.* (2008) used these coral and GPS data to estimate the spatial distribution of coupling along the megathrust assuming purely elastic deformation of the overlying and subducting plate and neglected any contribution from non-elastic deformation in the fore arc. They found that seismic slip for the last 300 yr accounts for only 21–41 per cent of slip on the megathrust. It is possible that a part of the slip might be accommodated by the backthrust. Further modelling is required to quantify the amount of slip that might be required to explain this discrepancy.

If we assume a fault surface of 180 × 15 km and a slip of 5 m, the seismic moment release would be 4.05×10^{20} N m, equivalent to a magnitude $M_w = 7.7$ earthquake along the slip plane assuming the rigidity $\mu = 3.0 \times 10^{10}$ N m^{-2}. If we assume a fault dip of 30°, the vertical uplift of the seafloor would be about 1.5 m on the backthrust. The total seismic energy released along the backthrust would be completely dwarfed by the immense energy released along the megathrust (being less than 2–5 per cent of the total seismic moment released), but would be of significant importance owing to its tsunamigenic potential. The slip along the backthrust during the earthquake might go unnoticed on the seismological record as it is near orthogonally oriented to the main thrust, where most of the rupture takes place releasing the majority of the earthquake energy. Simultaneous conjugate earthquake slip has been inferred in other instances (Robinson *et al.* 2001), and can be estimated allowing some of the slip on the orthogonal backthrust fault, in addition to the megathrust rupture plane.

In subduction zones, a hinge line is supposed to define the boundary between uplift and subsidence during coseismic and interseismic cycle (Sieh *et al.* 1999), and which also coincides with the down dip limit of the locked zone. The elastic dislocation model suggests that uplift occurs above the locked part of the plate interface and subsidence above the aseismic zone downwards during a coseismic event. On the other hand, the interseismic state (stress loading along the plate interface) is characterized by subsidence above the locked part and uplift above the aseismic zone. The zero vertical movement position lies at a constant distance from the subduction front and defines the hinge line. Natawidjaja *et al.* (2006, 2007) have used palaeogeodetic data (corals) to describe the pattern of uplift and subsidence for the last two centuries and of two major historical earthquakes in Mentawai region (in 1797 and 1833). However, the down-dip limit of the locked zone in the Sumatra region seems to extend further downwards (Simoes *et al.* 2004). The presence of the twin earthquakes on 2007 September 12 at 20 and 43 km depths (Konca *et al.* 2008) seems to suggest the the locked zone might be segmented in upper and lower locked zone, and the backthrust might be the boundary between two segments of the locked zone. Furthermore, the down-dip limit of the locked zone does not seem to be below the hinge line as is normally the case.

Two giant historical earthquakes occurred in 1797 (M_w 8.5–8.7) and in 1833 (M_w 8.6–8.9), which subsequently broke as much as 600 km section of the megathrust from 0.5°S to 3.2°S and from 2°S to as far as 5°S, respectively (Newcomb & McCann 1987; Natawidjaja *et al.* 2006). The 1797 earthquake produced a larger tsunami in Padang than the 1833 event. On the other hand, the 1833 tsunami was larger in Bengkulu. The tsunami-propagation model of the 1797 earthquake, based on the most reasonable scenario of the 1797 rupture (i.e. rupture length ∼400 km, slip ∼ up to 8 m) gives tsunami heights of no more than 3.5 m in Padang (Prawirodirdjo *et al.* 2000). Based on the historical account, the 1797 tsunami height observed in Padang could have been as high as 10 m (Natawidjaja *et al.* 2006) which is much higher than the model predicts. Hence, it is plausible that other factors, such as coincident back thrusting and landslides, might have enhanced the tsunami in Padang, and the mass wasting we observe on the NE margin of Siberut Island might have been produced during the 1797 earthquake thereby enhancing the tsunami. However, further study of the mass wasted material along the NE margin of the Mentawai Islands is required to corroborate these interpretations. Further north, the 2005 Nias-Simeulue earthquake did not excite a large tsunami. The obvious reason was because the 2005 event uplifted mostly the islands and surrounding shallow seas (Briggs *et al.* 2006). Interestingly, according to the historical notes, the predecessor of the 2005 earthquake that occurred in 1861 produced a reasonable size tsunami that killed many people in Nias and Simelue Islands (Newcomb & McCann 1987). Furthermore, the 1907 $M_w = 7.6$ Simeulue earthquake, the smallest of all, seems to have produced a greater tsunami than either the 1861 or 2005 earthquakes that occurred in the same area with likely similar source ruptures (Newcomb & McCann 1987). Therefore, it is possible that the 1907 tsunami might have been excited by movements on the backthrusts or by submarine landslides at the NE margin of Simeulue Island.

To explain the early arrival of tsunami (Plafker *et al.* 2006) in Banda Aceh during the 2004 earthquake, Chauhan *et al.* (2008) suggest that a 180 km wide backthrust might have ruptured coincidently with the megathrust. Since the backthrusts are nearly orthogonal to the megathrust, it would be difficult to detect them using either seismological or geodetic data. As the backthrusts are steeply dipping, they can produce a large vertical uplift, leading to

a large localized tsunami. Furthermore, a high vertical uplift along a backthrust coincidence with a megathrust earthquake will lead to an over estimation of the magnitude of past megathrust earthquakes based on coral data. If a backthrust slips aseismically, then interseismic subsidence and uplift would be perturbed. Natawidjaja *et al.* (2007) found a very large-scale (600 km) uplift and subsidence (1.5 m) of the Mentawai Islands in 1962, which would be equivalent to an earthquake of magnitude 8.4 if the slip was along the megathrust. There were several other small episodes of uplift and subsidence in 1968, 1975 and 1984. It is possible that some of these anomalies could have been associated with movement along the backthrusts observed at the NE margin of Mentawai Island instead of the megathrust, which is usually assumed.

The presence of islands and ridges along the Sumatra subduction zone remains an enigma. One possibility is that the islands consist of old accretionary wedge (Kopp *et al.* 2002) and hence have been uplifted. Singh *et al.* (2008) suggest that underplatting of sliced oceanic crust would uplift the islands; the existence of ophiolites and high gravity anomalies on the Islands (Samuel *et al.* 1997) support this hypothesis. The presence of backthrusting at the NE margin of islands and ridges would further reinforce the uplift of Islands and would keep them subaerial.

7 CONCLUDING REMARKS

There are several large cities along the west coast of Sumatra with a very large population living at 5–6 m above the sea level. The Siberut section of the megathrust has not had any large earthquakes since 1797, and hence it is likely to break in the near future (Nalbant *et al.* 2006; Konca *et al.* 2008; Sieh *et al.* 2008). Recent geodetic studies suggest that up to 8 m of slip has been accumulated along this segment of the megathrust (Chlieh *et al.* 2008). Konca *et al.* (2008) argue that only partial energy has been released during the 2007 earthquake sequence and a significant section of the Mentawai segment may rupture in the very near future. Since the coastal region of mainland western Sumatra is to a large extent protected by the Mentawai Islands and outerarc highs (McCloskey *et al.* 2008) the tsunami risk to this region could be due to the megathrust that produces tsunami towards the ocean side of the Mentawai Islands as well as due to the backthrusts NE of Mentawai Islands. McCloskey *et al.* (2008) show that it would take about 32 min for a tsunami to arrive near the coast of western Sumatra if it were produced by a rupture on the megathrust. However, if a tsunami was produced by the backthrust, it would arrive in 20 min in Padang. Borrero *et al.* (2009) have carried out extensive field work and modelling of tsunami after the 2007 earthquake. They report that the residence of Pantai Jakat, near Bengkulu, observed the first tsunami wave arrival after 15 min of the earthquake, then withdrew before returning an hour later. This early arrival could be due to some other factors, such as slip on a local backthrust and/or landslides. Only a few percent of energy released along the backthrust could have a devastating effect. Therefore, measures should be taken to mitigate tsunami risk generated by these backthrusts and landslides.

Such backthrusts may be present further north, in the Nicobar and Andaman Island region, and may produce some large localized tsunami in the Andaman Sea. Chauhan *et al.* (2008) show that high run-up values and early arrival of tsunami on 2004 December 26 in northern Sumatra can be explained by a localized tsunami source due to a re-activation of a backthrust coincident with the main megathrust event. These observations suggest that the presence of a backthrust in an oblique subduction zone could be a norm rather than an exception, and hence they may play a more important role in tsunami generation than it has been realized so far, and therefore, they should be taken into account for seismological and tsunami modelling studies and risk mitigation during the great thrust earthquakes.

ACKNOWLEDGMENTS

The Pre-TIGap survey was funded by the French Ministry of Foreign Affairs as a contribution to Indonesian-French collaboration for earthquake and tsunami study. LIPI provided all the logistics for the survey. NH and AH were funded by the French Ministry of Foreign Affairs and AC is funded by the French Ministry of Research Doctoral Fellowship. This is IPG Paris contribution 2574.

REFERENCES

Bellier, O., Bellon, H., Sébriera, M., Sutanto, & Maury, R.C., 1999. K Ar age of the Ranau Tuffs: implications for the Ranau caldera emplacement and slip-partitioning in Sumatra (Indonesia), *Tectonophysics,* **312**(2–4), 347–359.

Borrero, J.C., Weiss, R., Okal, E.A, Hidayat, R., Suranto, Arcas, D. & Titov, V.V., 2009. The tsunami of 2007 September 12, Bengkulu province, Sumatra, Indonesia: post-tsunami field survey and numerical modelling, *Geophys. J. Int.,* **178,** 180–194.

Briggs, R.W. *et al.*, 2006. Deformation and slip along the Sunda megathrust in the great 2005 Nias-Simeulue earthquake, *Science,* **311,** 1897–1901.

Chauhan, A., Singh, S., Hananto, N., Carton, H., Dessa, J.-X., Klingelhoefer, F., Permana, H. & Graindorge, D., 2008. Forearc backthrusting as a source of 26 December 2004 Sumatra-Andaman tsunami, *EOS, Trans. Am. geophys. Un.,* **89,** Fall Meet. Suppl. Abstract U51–004.

Chauhan, A.S. *et al.*, 2009. Seismic imaging of forearc backthrusts at northern Sumatra subduction zone, *Geophys. J. Int.,* **179,** 1772–1780, doi:10.1111/j.1365-246X.2009.04378.x.

Chlieh, M., Avouac, J.-P., Sieh, K., Natawidjaja, D.H. & Galetzka, J., 2008. Investigation of interseismic strain accumulation along the Sunda megathrust, offshore Sumatra, *J. geophys. Res.,* **113,** B05305, doi:10.1029/2007JB004981.

Diament, M. *et al.*, 1992. Mentawai fault zone off Sumatra—a new key to the geodynamics of western Indonesia, *Geology,* **20,** 259–262.

Engdahl, E.R., Villasenor, A., DeShon, H.R. & Thurber, C.H., 2007. Teleseismic relocation and assessment of seismicity (1918–2005) in the region of the 2004 Mw 9.0 Sumatra-Andaman and 2005 Mw 8.6 Nias Island Great Earthquakes, *Bull. seism. Soc. Am.,* **97**(1A), S43–S61.

Fitch, T., 1972. Plate convergence, transcurrent faults, and internal deformation adjacent to southeast asia and the western Pacific, *J. geophys. Res.,* **77,** 4432–4462.

Graindorge, D. *et al.*, 2008. Impact of lower plate structure on upper plate deformation at the NW Sumatran convergent margin from seafloor morphology, *Earth planet. Sci. Lett.,* **275,** 201–210.

Konca, A.O. *et al.*, 2008. Partial rupture of a locked patch of the Sumatra megathrust during the 2007 earthquake sequence, *Nature,* **456,** 631–635.

Kopp, H., Flueh, E., Klaeschen, D., Bialas, J. & Reichert, C., 2001. Crustal structure of the central Sunda margin at the onset of oblique subduction, *Geophys. J. Int.,* **147,** 449–474.

Lorito, S., Romano, F., Piatanesi, A. & Boschi, E., 2008. Source process of the September 12, 2007 Mw 8.4 Southern Sumatra earthquake from tsunami tide gauge record inversion, *Geophys. Res. Lett.,* **35,** L02310, doi:10.1029/2007GL032661.

McCaffrey, R., Zwick, P.C., Bock, Y., Prawirodirdjo, L., Genrich, J.F., Stevens, C.W., Puntodewo, S.S.O. & Subarya, C., 2000. Strain partitioning during oblique plate convergence in northern Sumatra: geodetic and seismologic constraints and numerical modelling, *J. geophys. Res.,* **105,** 28 363–328 376.

McCloskey, J., Antonioli, A., Piatanesi, A. & Sieh, K., 2008. Tsunami threat in the Indian Ocean from a future megathrust earthquake west of Sumatra, *Earth planet. Sci. Lett.,* **265,** 61–81.

Mosher, D.C., Austin, J.A., Fisher, D. & Gulick, S.P.S., 2008. Deformation of the northern Sumatra accretionary prism from high-resolution seismic reflection profiles and ROV observations, *Marine Geol.,* **252,** 89–99.

Nalbant, S., Steacy, S., Sieh, K., Natawidjaja, D. & McCloskey, D., 2006, Earthquake risk on the Sunda trench, *Nature,* **435,** 757–758.

Natawidjaja, D.H., Sieh, K., Galetzka, J., Suwargadi, B., Cheng, H. & Edwards, R.L., 2006. Source Parameters of the great Sumatran megathrust earthquakes of 1797 and 1833 inferred from coral microatolls, *J. geophys. Res.,* **111,** 147–227.

Natawidjaja, D.H., Sieh, K., Galetzka, J., Suwargadi, B., Cheng, H., Edwards, R.L. & Chlieh, M., 2007. Interseismic deformation above the Sunda megathrust recorded in coral microatolls of the Mentawai Islands, West Sumatra, *J. geophys. Res.,* **112,** B02404, doi:10.1029/2006JB004450.

Newcomb, K.R. & McCann, W.R., 1987. Seismic history and seismotectonics of the Sunda Arc, *J. geophys. Res.,* **92,** 421–439.

Plafker, G., Nishenko, S., Cluff, L. & Syahrial, M., 2006. The Cataclysmic 2004 Tsunami on NW Sumatra—preliminary evidence for a near-field secondary source along the western Aceh Basin, *Seism. Res. Lett.,* **77,** 426.

Prawirodirdjo, L., 2000. A geodetic study of Sumatra and the Indonesian region: kinematics and crustal deformation from GPS and triangulation, *PhD thesis*, University of California, San Diego, San Diego.

Prawirodirdjo, L., Bock, Y., Genrich, J.F., Puntodewo, S.S.O., Rais, J., Subarya, C. & Sutisna, S., 2000. One century of tectonic deformation along the Sumatran fault from triangulation and Global Positioning System surveys, *J. geophys. Res.,* **105,** 6779–6796.

Robinson, D.P., Henry, C., Das, S. & Woodhouse, J.H., 2001. Simultaneous rupture along two conjugate planes of the Wharton Basin earthquake, *Science,* **292,** 1145–1148.

Samuel, M.A., Harbury, N.A, Bakri, A., Banner, F.T. & Hartono, L., 1997. A new stratigraphy for the Islands of the Sumatran Arc, Indonesia. *J. SE Asian Earth Sci.,* **15,** 339–380.

Schluter, H.U, Gaedicke, C., Roeser, H.A., Schreckenberger, B., Meyer, H., Reichert, C., Djajadihardja, Y. & Prexl, A., 2002. Tectonic features of the southern Sumatra-western Java forearc of Indonesia, *Tectonics,* **21**(5), 11.1–11.15.

Seeber, L., Mueller, C., Fujiwara, T., Arai, K., Soh, W., Djajadihardja, Y.S. & Cormier, M.-H., 2007. Accretion, mass wasting, and partitioned strain over the 26 Dec 2004 Mw = 9.2 rupture offshore Aceh, northern Sumatra, *Earth planet. Sci. Lett.,* **263,** 16–31.

Sibuet, J.-C. *et al.*, 2007. 26th December 2004 great Sumatra-Andaman earthquake: co-seismic and post-seismic motions in northern Sumatra, *Earth planet. Sci. Lett.,* **263,** 88–103.

Sieh, K. & Natawidjaja, D., 2000. Neotectonics of the Sumatran fault, Indonesia, *J. geophys. Res.,* **105,** 28 295–228 326.

Sieh, K., Ward, S.N., Natawidjaja, D. & Suwargadi, B.W., 1999. Crustal deformation at the Sumatran subduction zone revealed by coral rings, *Geophys. Res. Lett.,* **26,** 3141–3144.

Sieh, K. *et al.*, 2008. Earthquake supercycles inferred from sea-level changes recorded in the corals of West Sumatra, *Science* **322,** 1674–1678.

Simoes, M., Avouac, J.P., Cattin, R. & Henry, P., 2004. Sumatra subduction zone: a case for a locked fault zone extending into the mantle, *J. geophys. Res.,* **109,** B10402, 1–16.

Singh, S.C. *et al.*, 2005. Sumatra earthquake research indicates why rupture propagated northward, *EOS, Trans. Am. geophys. Un.,* **86**(48), 497.

Singh, S.C. *et al.*, 2008. Seismic evidence for broken oceanic crust in the 2004 Sumatra earthquake epicentral region, *Nat. Geosci.,* **1**(11), 771–781.